

Journal of Biomedical Optics

SPIEDigitalLibrary.org/jbo

Temperature dependence of the optoacoustic transformation efficiency in *ex vivo* tissues for application in monitoring thermal therapies

Sergey M. Nikitin
Tatiana D. Khokhlova
Ivan M. Pelivanov

Temperature dependence of the optoacoustic transformation efficiency in *ex vivo* tissues for application in monitoring thermal therapies

Sergey M. Nikitin, Tatiana D. Khokhlova, and Ivan M. Pelivanov

International Laser Center, M.V. Lomonosov Moscow State University, Moscow, Russia

Abstract. The calibration dependencies of the optoacoustic (OA) transformation efficiency on tissue temperature are obtained for the application in OA temperature monitoring during thermal therapies. Accurate measurement of the OA signal amplitude versus temperature is performed in different *ex vivo* tissues in the temperature range 25°C to 80°C. The investigated tissues were selected to represent different structural components: chicken breast (skeletal muscle), porcine lard (fatty tissue), and porcine liver (richly perfused tissue). Backward mode of the OA signal detection and a narrow probe laser beam were used in the experiments to avoid the influence of changes in light scattering with tissue coagulation on the OA signal amplitude. Measurements were performed in heating and cooling regimes. Characteristic behavior of the OA signal amplitude temperature dependences in different temperature ranges were described in terms of changes in different structural components of the tissue samples. The accuracy of temperature reconstruction from the obtained calibration dependencies for the investigated tissue types is evaluated. © 2012 Society of Photo-Optical Instrumentation Engineers (SPIE). [DOI: 10.1117/1.JBO.17.6.061214]

Keywords: optoacoustics; photoacoustics; high-intensity focused ultrasound; temperature monitoring; transformation efficiency.

Paper 11483SS received Sep. 5, 2011; revised manuscript received Jan. 7, 2012; accepted for publication Feb. 1, 2012; published online May 14, 2012.

1 Introduction

Accurate, rapid, and noninvasive measurement of temperature distribution inside biological tissues is an important issue in most thermal therapies aiming at localized tumor destruction, such as hyperthermia, high-intensity focused ultrasound (HIFU) therapy, laser interstitial thermotherapy (LITT), and radio frequency (RF) ablation.

In HIFU therapy, powerful ultrasound waves are focused inside a human body to induce thermal denaturation of tissue at the focus of the transducer without affecting the surrounding organs. HIFU ablation has been applied to the treatment of a wide variety of both benign and malignant tumors, including uterine fibroids, prostate cancer, liver tumors, and other solid tumors that are accessible to ultrasound energy.¹⁻⁴ A single HIFU lesion is often referred to as being “cigar-shaped,” and is typically about 5 to 10 mm in length, 2 to 3 mm in cross section, and takes anywhere from 1 ms to tens of seconds to induce, depending on the clinical application. For the treatment of a larger tissue volume, the transducer focus is scanned over the targeted area.

Both RF ablation and LITT are minimally invasive procedures in which either an optical fiber or a needle electrode is inserted into the targeted tissue area under ultrasound or magnetic resonance (MR) guidance. The unwanted tissue adjacent to the tip of the fiber or electrode is then thermally coagulated through either light absorption or heat generated by high-frequency alternating current. A single treatment takes several minutes, and the resulting lesion can be 5 to 10 mm in diameter.⁵

Based on the time needed to create a single thermal lesion and the lesion size, the requirement to the temporal resolution of a temperature-monitoring method should be on the order of a second or less, and the spatial resolution should be within a millimeter range. To date, the following methods have been employed for this purpose, with varying degrees of success: diagnostic ultrasound-based methods, MR thermometry, infrared thermography, and acousto-optical imaging.

Most diagnostic ultrasound-based methods for temperature monitoring use the temperature dependence of the sound speed in tissue.⁶ This dependence leads to a shift of the heated area relative to the image of the targeted tissue. Solving the inverse problem under the approximation of an acoustically homogeneous medium, the temperature distribution within the tissue can be reconstructed,^{7,8} provided that the dependence of sound speed on temperature for this tissue is known. The essential limitation of this method is that most tissues cannot be considered acoustically homogeneous. In addition, the dependence of the speed of sound on temperature is relatively weak (~1 m/s per degree) and varies greatly among tissues.^{9,10} For example, the speed of sound increases with temperature in muscle and other tissues with high water content and decreases in fatty tissues.^{6,11-13} Structural tissue changes caused by coagulation or dehydration also lead to changes in the speed of sound,¹³ but the total change does not exceed a few percent for all kinds of soft tissues in the temperature range of 30°C to 80°C.¹¹

The biggest advantage of MR thermometry is that, unlike ultrasound-based methods, it can provide tissue temperature maps overlying the MR image of the target almost in real time. The distribution of sufficient thermal dose is then calculated and assumed to correspond to thermally ablated tissue. The temporal

Address all correspondence to: Ivan M. Pelivanov, International Laser Center, M.V. Lomonosov Moscow State University, Moscow, Russia. Tel: +7495 939 5309; Fax: +7495 939 3113; E-mail: pelivanov@ilc.edu.ru.

resolution of MR thermometry is 1 to 4 s per image, and the spatial resolution is determined by the size of the image voxel, which is typically about $2 \times 2 \times 6 \text{ mm}^3$.¹⁴ Therefore, MR-guided HIFU or LITT is suitable only for treatments in which the heating occurs slowly, on the order of tens of seconds for a single thermal lesion. Motion artifacts due to breathing and heartbeat are also a concern in a clinical setting. MR-guided HIFU has been used clinically for the treatment of breast tumors^{15,16} and uterine fibroids,¹⁷ and MR-guided LITT for treatment of brain, liver, and prostate tumors.¹⁸ The practical limitations are the high cost and limited availability of MR imaging systems.¹⁹ Unfortunately, neither MR imaging nor ultrasound-based guidance methods can provide the image of the thermal lesion directly and in real time as it forms in tissue, due to the lack of contrast between intact and thermally denatured tissue.

Infrared thermography allows for performing temperature monitoring in real time within 0.1°C , but only at the surface of an object, and it is therefore only applicable for photodynamic therapy of skin or mucous tissue.²⁰

Optical imaging methods, such as optical diffusion tomography (ODT), seem attractive for imaging thermal lesions since coagulation necrosis induces large changes, up to 300%, in optical properties of tissue containing blood and protein.^{21–26} However, strong light scattering inherent to most tissues in the visible and near-infrared range dramatically decreases the image spatial resolution,²⁷ which is comparable to the imaging depth. Since thermal therapy procedures are often applied to tissues located at the depth of several centimeters within a human body, and a typical size of a thermal lesion is on the order of millimeters, purely optical methods are hardly applicable for the purpose, despite the advantage of high contrast.

The acousto-optical method^{28,29} is a hybrid and is based on the modulation of diffuse light in tissue by ultrasound waves emitted by conventional ultrasound scanners. Only ultrasound-modulated photons are then used for image reconstruction; therefore, the spatial resolution is determined by the area of interaction of light and sound; i.e., the focal area of the ultrasound array. Sufficient sensitivity of this method for detection of lesion formation *in vitro* was demonstrated.²⁹ However, even in 2-D environments, the acousto-optical method faces substantial difficulties in lesion imaging and temperature monitoring.

Thus, the development of a noninvasive method that would have sufficient spatial and temporal resolution, high sensitivity to temperature change, high contrast between intact and thermally denatured tissue, and sufficient monitoring depth (a few centimeters) is of great practical importance.

Optoacoustic (OA) imaging is a potentially advantageous method for both imaging thermal lesions and measuring temperature distribution inside tissue. In OA imaging, tissue is irradiated by a nanosecond laser pulse, which leads to tissue heating, its rapid thermal expansion, and generation of a wideband ultrasound signal that will be referred to as the “OA signal.”³⁰ The OA signals are then detected by an array of ultrasound transducers and used for the tomographic reconstruction of the distribution of laser-induced heat release in tissue.^{31–33} The amplitude of the OA signal excited in an elementary tissue volume is proportional to the efficiency of the OA transformation—the product of light absorption coefficient μ_a and the Grueneisen parameter Γ , calculated as $\Gamma = c_0^2\beta/c_p$ (where c_0 is sound speed, c_p is specific heat, and β is the thermal

expansion coefficient).³⁰ Both μ_a and Γ depend on structural changes that occur in tissue during its heating.^{10,11,24,34–38}

As mentioned above, the temperature changes of the speed of sound in most soft tissues do not exceed a few percent. The variation of the specific heat of tissues with temperature is explored very little, especially beyond the point of tissue coagulation. The only known example is liver tissue that exhibits changes in specific heat by no more than a few percent in the temperature range of 20°C to 80°C .³⁷ This is not surprising, considering that the specific heat of water changes within 1 percent in that temperature range.¹⁰ However, the variations in c_p of fatty tissues with temperature may be more significant.¹⁰

The thermal expansion coefficient of water increases by 5% per degree; therefore, the corresponding dependence in tissues with high water content may be quite strong. Unfortunately, the literature yields very little information on the temperature dependence of β in different tissues for temperatures over 40°C . Some authors consider β a constant up to the point of tissue coagulation;³⁹ beyond that point, the change in β , to our knowledge, was not investigated to date.

The information on the dependence of μ_a on tissue coagulation status is also contradictory. Optical properties (at 632 nm wavelength) of *ex vivo* myocardial tissue samples, which were subjected to rapid step changes in temperature, were studied by Agah et al.²⁴ After the temperature had reached the maximum value of about 52°C , the light absorption coefficient increased by 1.5 times compared to its initial value. More than twofold growth in light absorption was detected at 1064 nm for *ex vivo* porcine liver²¹ and chicken breast²³ samples after thermal denaturation. The increase in optical absorption by 100% to 300% within the wavelength range of 600 to 1500 nm was also demonstrated after *in vivo* rat liver coagulation.²² Such an increase can be explained by the fact that the coagulation changes the concentration of chromophores^{40,41} and by formation of methemoglobin from hemoglobin in blood at temperatures beyond 60°C .^{36,42} In contrast to the works cited above, a sufficient decrease of light absorption for human and porcine liver samples during heating from 36°C to 80°C was observed by Ritz et al.^{35,43} This result could be related to the complex procedure of sample preparation, which included sample freezing in liquid nitrogen and subsequent homogenization. We believe, however, that the growth in light absorption coefficient, rather than its decrease after tissue denaturation, is more explicable for most types of soft tissues.

Thus, temperature changes in the efficiency of OA conversion (the product of μ_a and Γ) seems to be much greater than that of the speed of sound or acoustic impedance. That makes the OA technique very promising for temperature monitoring in biological tissues. Both the image of the thermal lesion and the temperature distribution inside the tissue can potentially be acquired by solving the inverse OA imaging problem. However, for direct application of the OA method, the dependence $\Gamma(T)$ and the change in μ_a with coagulation should be known in the tissue under examination. The corresponding calibration measurements were addressed in several works that are reviewed briefly below.

The feasibility of the OA method in diagnostics of an isolated thermal lesion was first demonstrated by Khokhlova et al.²¹ for a HIFU-induced thermal lesion in porcine liver, and by Larin et al.⁴⁴ for an LITT-induced lesion in canine liver. In both cases, the lesions were induced at 1 cm depth, and the sizes were $3 \text{ mm} \times 25 \text{ mm}$ for the HIFU lesion and $5 \text{ mm} \times 15 \text{ mm}$ for

the LITT lesion. The profiles of the OA signals generated in the samples and detected by single-element transducers clearly indicated the presence of a highly absorbing heterogeneity—the thermal lesion—and allowed the determination of its transverse size and location depth. In a separate set of experiments, the contrast in optical absorption at an 1064-nm wavelength between coagulated and intact porcine liver tissue was measured and was 250% for porcine liver²¹ and 150% for canine liver tissue.⁴⁴ The difference in these values is most probably related to the difference of the measurement methods or the procedures for sample preparation employed in the studies.

In another study, HIFU lesions were produced in *in vivo* and *ex vivo* mouse kidney and then examined using an OA imaging system.⁴⁵ Surprisingly, the lesion appeared darker on the OA image (i.e., less absorptive than the intact tissue) in the *in vivo* case, but brighter in the *ex vivo* case. The reason for such behavior was unclear, but the authors speculate that despite the expected growth of the light absorption coefficient, the coagulation process in tissue can block blood circulation and initiate tissue dehydration. These processes are assumed to decrease the thermal expansion coefficient and, consequently, the amplitude of the OA signal from the lesion.

The dependencies of the OA signal amplitude on temperature were measured by Larin et al. in canine liver and canine muscle tissue.⁴⁴ The increase in OA pressure amplitude with tissue heating was observed before tissue coagulation apparently due to the gradual increase of the thermal expansion coefficient. After tissue coagulation occurred, the increase became more rapid, possibly due to abrupt change in tissue optical absorption and scattering. Unfortunately, the influence of each individual parameter (absorption, scattering, and Gruneisen parameter) on the signal amplitude could not be separated in that particular experimental design.

In other studies, the dependence of the OA signal amplitude on temperature was measured in turkey muscle⁴⁶ and porcine muscle tissue infused with gold nanoparticles.⁴⁷ The experiments were performed in a relatively narrow temperature range (23°C to 37°C), and a linear relationship was found in both cases.

The goal of the present work was to investigate the temperature dependence of the OA transformation efficiency at different heating-cooling regimes, in a wide range of temperatures, and in different tissue types to evaluate the applicability of OA imaging to temperature mapping during thermal therapies.

2 Materials and Methods

2.1 Theoretical Background

The reconstruction of the temperature distribution in tissue by solving the inverse problem of OA tomography is possible if the calibration dependence $\mu_a\Gamma$ on temperature for that tissue is known. In the present work, the following method is employed to measure the calibration curves.

Consider the laser beam irradiating the boundary $z = 0$ of the transparent medium and the biological tissue. The laser fluence in the incident laser beam can be represented as

$$E_{\text{inc}}(r_{\perp}, \tau) = E_0 L(\tau) R(r_{\perp}), \quad (1)$$

where $R(r_{\perp})$ and $L(\tau)$ are the dimensionless transverse fluence distribution within the laser beam and the temporal profile of the laser pulse, correspondingly. For simplicity, the distribution $R(r_{\perp})$ will be considered Gaussian, as follows:

$$R(r_{\perp}) = \exp\left(-\frac{4r_{\perp}^2}{d^2}\right), \quad (2)$$

where d is the laser beam diameter. Within the turbid medium (i.e., tissue), the axial distribution of laser fluence can be represented as

$$E(z, r_{\perp} = 0, \tau) = E(z)L(\tau). \quad (3)$$

If the laser pulse is considered infinitely short, $L(\tau) = \tau_L \delta(\tau)$, the heating of the turbid medium can be considered instantaneous, and hence the thermal sources as “frozen.” The profile of the OA signal excited in the turbid medium and detected in backward mode in the transparent medium, but very close to the tissue surface, can be represented as^{48,49}

$$p_0(\tau, r_{\perp} = 0) = \begin{cases} 0, & \tau < 0 \\ R_{ac}\Gamma\mu_a E(z = c_{tr}\tau), & \tau > 0 \end{cases}, \quad (4)$$

where $R_{ac} = 2\rho_{tr}c_{tr}/(\rho_{tr}c_{tr} + \rho_0c_0)$; ρ_{tr} and ρ_0 , are the density of the transparent and turbid media, respectively; and c_{tr} is the speed of sound in the transparent medium. As seen, the temporal profile of the acoustic signal described by Eq. (4) in the region $\tau > 0$ corresponds to the in-depth distribution of heat release.

In the case of a short, but finite, laser pulse ($\mu_{\text{eff}}c_0\tau_L \ll 1$), it is necessary to take into account the change of the heat release distribution within the laser pulse duration, which results in the broadening of the OA signal front:

$$p(\tau, r_{\perp} = 0) = R_{ac}\Gamma\mu_a \int_0^{\infty} L(t)I[c_{tr}(\tau - t)]\vartheta(\tau - t)dt, \quad (5)$$

where $\vartheta(\tau)$ is the Heaviside function and $I(z)$ is the laser fluence rate in the turbid medium.

Equation (5) shows that the amplitude of the OA signal excited in a turbid medium is proportional to $\mu_a\Gamma$, but it also depends on the distribution of laser fluence $E(z)$ within the medium. It is well known that the laser fluence in the subsurface region can exceed the value of E_0 in the incident laser beam by up to six times due to backscattering.^{50,51} The amplification factor $k = E_{\text{max}}/E_0$ depends on the ratio μ_a/μ'_s of tissue optical coefficients and on the value of d/l^* ($l^* = 1/\mu'_s$, photon transport mean free path in the turbid medium).⁵² This factor is difficult to account for in the measurements when the optical coefficients are not known beforehand or can change unexpectedly in the course of the experiment. However, if a narrow laser beam is employed (i.e., $d/l^* \ll 1$), the subsurface laser fluence amplification diminishes ($k \rightarrow 1$) and the laser fluence is at its maximum at the tissue surface: $E_{\text{max}} = E(z = 0)$. The OA signal amplitude thus depends on μ_a only, not on the ratio of optical coefficients μ_a/μ'_s .⁵² However, in this case, a strong diffraction transformation of the acoustic signals within the transparent medium takes place,⁵³ and the signal profile, detected in the transparent medium at the distance L from the tissue surface, is represented as follows:

$$p_d(\tau, r_{\perp} = 0) = \frac{d^2}{8c_{tr}L} \frac{\partial p}{\partial \tau} = \frac{d^2}{8c_{tr}L} R_{ac}\Gamma\mu_a \left[\frac{I_0}{E_0} E(z = 0)L(\tau) + \frac{\partial E(c_{tr}\tau)}{\partial \tau} \vartheta(\tau) \right], \quad (6)$$

and is essentially the time derivative of Eq. (5).

The first component of Eq. (6) repeats the laser pulse envelope and has a sharp maximum at $\tau = 0$. Since the laser fluence distribution $E(z)$ inside a turbid medium is a smoothly varying function compared to the laser pulse envelope, the second component of Eq. (6) is much smaller than the first one within the laser pulse duration. Therefore, the leading edge of the OA signal $p(\tau < 0)$ is determined by the laser pulse envelope, and its amplitude is proportional to the light absorption coefficient μ_a and to the maximal value of laser fluence E_{\max} in the medium that depends very little on the reduced scattering coefficient μ'_s .⁵² The trailing edge of the OA signal profile is determined by the two terms of Eq. (6) and depends on the distribution $E(z)$ and, therefore, on both coefficients μ_a and μ'_s .

Thus, the OA conversion coefficient $\mu_a\Gamma$ in tissue and its dependence on temperature and tissue coagulation status can be measured locally from the amplitude of the OA signal excited in tissue by a narrow laser beam under stress confinement and thermal confinement conditions. The inaccuracy of measurement of $\mu_a\Gamma$ in this case will not exceed 8%, even if the reduced scattering coefficient μ'_s is changed twice due to tissue denaturation.⁵²

2.2 Experimental Setup

The diagram of the experimental setup is shown in Fig. 1. Radiation of the fundamental harmonic (laser wavelength $\lambda = 1064$ nm, pulse duration $\tau_L = 12$ ns, pulse repetition rate 50 Hz) of a Q-switched Nd:YAG laser was used for the excitation of the OA signals. The pulse energy could be decreased by a set of neutral light filters and was 2 to 3 mJ at the tissue surface. The laser beam diameter at the tissue surface was 2.5 mm. It is important to note that the incident laser fluence was lower than medical safety standards dictate.⁵⁴ Heating of the tissue samples by a single laser pulse was less than one-hundredth of a degree, which can be estimated by a simple expression:

$$\Delta T = \mu_a E_0 / \rho c_p \approx \frac{20 \text{ m}^{-1} * 600 \text{ J/m}^2}{1000 \text{ kg/m}^3 * 4200 \text{ J/K}} = 0.0028 \text{ K.} \quad (7)$$

Here, the density and specific heat are that of water. In some tissues, these values may be different by no more than 20%, which would lead to an insubstantial difference in the estimated

temperature increment.¹⁰ However, even neglecting heat diffusion, the accumulated laser-induced heating of the sample over the entire cycle of 128 laser pulses did not exceed 0.4 K. This allowed the tissue heating effects induced by probe laser radiation to be disregarded.

A light-separating cube with a 4-cm side was used for rotation of the laser beam by 90 deg toward the tissue surface. The cube was made of the two quartz prisms of triangular cross-section brought into optical contact. A thin metal layer was deposited onto one of the contacting surfaces. This layer was "acoustically thin," i.e., the OA signal excited in the medium passed through the contact layer without considerable reflection losses. As shown in Fig. 1, the bottom of the cube was in acoustical contact with the investigated tissue. The top of the cube was attached to a 7-mm-thick duralumin diaphragm filled with deionized water, which was in acoustic contact with the receiving custom-built piezoelectric transducer. The transducer itself had a metal housing fixed in a metal holder placed on the massive optical table. The presence of the duralumin diaphragm with water and the metal holder provided dissipation of heat, and thereby sufficient decrease of temperature, at the detector surface during the experiment (the maximum temperature of deionized water adjacent to the detector was additionally monitored with a thermocouple and did not exceed 40°C). Possible changes in detector sensitivity with temperatures in the range of 25°C to 40°C were tested by detecting the signal from a well-characterized OA source—the blue-green glass light filter BGG-22. No changes in the transducer spectral sensitivity exceeding 1% were observed. Thus, the pyroelectric effect in the piezoelement of the transducer and the change in its sensitivity with temperature were disregarded.

The detector was made of a 110- μm -thick polyvinylidene fluoride foil (PVDF) film deposited onto a block of PMMA. It had a smooth frequency response in the megahertz range, and its low-frequency sensitivity was 845 mV/Pa (after a 50-fold amplification). A more detailed description of the receiver design can be found in our previous works.^{21,52,55} The detected signal was recorded by a digital oscilloscope (Tektronix TDS-1012, sampling rate 1 GHz, analog frequency 100 MHz) online with a computer.

The temperature dependence of OA conversion efficiency can be very different for tissues with different structural components, i.e., the content of fat, water, protein, and blood.^{10,11,36}

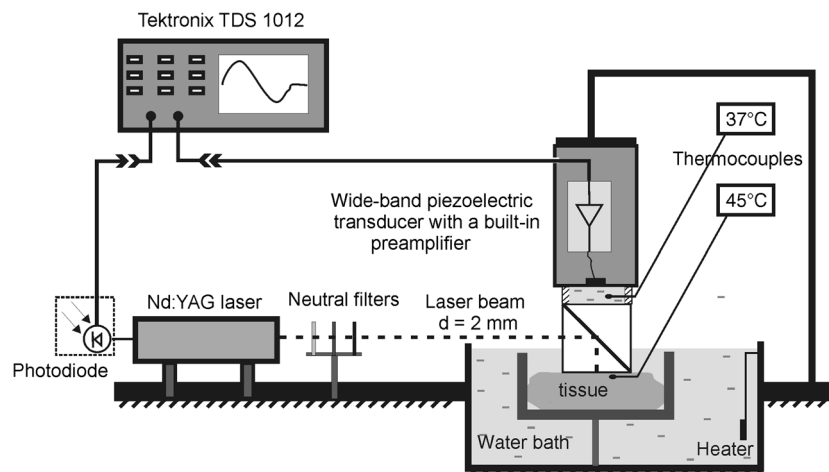


Fig. 1 Diagram of the experimental setup.

For that reason, we selected several representative tissues for the measurements: chicken breast as a model of skeletal muscle, porcine lard as a model of fatty tissue, and porcine liver as a model of richly perfused tissue. The investigated tissues were obtained from an abattoir and stored on ice for no longer than 36 h after removal from the animal. The samples were cut out to fit a holder with dimensions of $3 \times 3 \times 2$ cm and then degassed in a desiccant chamber for 1 h. This allowed the extraction of air bubbles from tissue that could distort the temporal profile of the OA signals. Overall, 10 samples of each tissue type were tested.

Following the degassing procedure, the samples were mounted in the holder, which was then placed into a bath filled with heated, deionized water. Tissue temperature was monitored with a thermocouple. Measurement of the temperature dependencies of the OA signal amplitude was performed in two regimes: heating and cooling. During both heating and cooling, the temperature of samples was changed in the range 23°C to 78°C . For several samples of each tissue type, the cooling process was also performed starting from lower temperatures to evaluate residual changes in tissue properties. Temperature change was very slow—about 2 min per degree—to provide near-homogeneous temperature distribution²⁴ within the tissue samples. To perform measurements in the cooling regime, water in the thermostat was gradually mixed with cold water.

3 Results

Typical temporal profiles of the detected OA signals at different tissue temperatures for porcine liver and fatty tissues are shown in Fig. 2(a) and 2(b). As seen in Fig. 2(a), the amplitude of the OA signal from porcine liver almost doubles as the temperature increases from 31°C to 76°C , whereas in porcine lard it

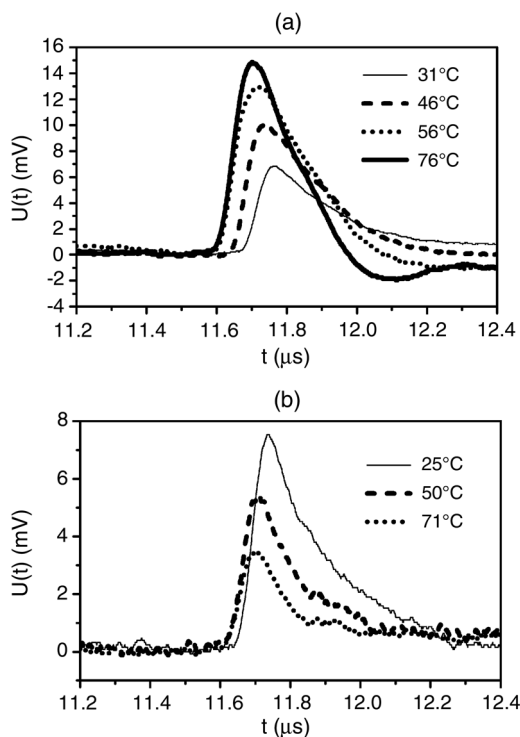


Fig. 2 Temporal profiles of the OA signals excited in porcine liver (a) and lard (b) tissue samples at different temperatures and detected in backward mode, in the far field by the wide-band piezoelectric transducer.

decreases significantly with temperature. As discussed above, the trailing edge of the OA signal excited at a narrow laser beam cannot be used for quantitative determination of μ_{eff} in tissue due to the laser beam divergence in tissue and OA signal diffraction transformation. However, the slope of the trailing edge can qualitatively indicate changes in optical properties: the steepening of the slope can be caused by the increase of μ_a , μ_s' , or both. Figure 2 demonstrates the different dynamics of changes in the trailing edge slopes for the different tissues. In porcine liver [Fig. 2(a)], the slope steepness does not change with temperature until partial coagulation starts to occur at $\sim 46^\circ\text{C}$ and within the interval 65°C to 72°C . Gradual steepening of the slope occurs with the increase in temperature in the ranges 46°C to 65°C and 72°C to 76°C , indicating the increase of optical coefficients. The potential reasons for this fact will be considered in the discussion. Similar changes in the signal slope were observed for the chicken breast samples. However, in porcine lard [Fig. 2(b)], the OA signal profile changed very little with temperature, except for the decrease in amplitude. This indicates the absence of considerable changes in tissue absorption and scattering.

3.1 Temperature Dependence of the OA Signal Amplitude in Chicken Breast

A typical temperature dependence of the OA signal amplitude for a chicken breast sample is shown in Fig. 3. The dependence during the heating process consists of three parts: a linear dependence preceding tissue coagulation (23°C to 45°C); a steeper linear dependence corresponding to the coagulation process, and, apparently, to the changes in thermophysical and optical properties (46°C to 65°C); and a post-coagulation part ($>65^\circ\text{C}$), in which very little change of the signal amplitude with temperature is observed.

When cooling of a sample started from temperatures below 46°C , the dependence repeated the heating curve in the inverse direction (shown by the solid circles in Fig. 3), which means that no irreversible changes in tissue structure occur. When the cooling process started from temperatures above 46°C , the OA signal amplitude did not return to its initial value at room temperature (shown by solid triangles and squares in Fig. 3), revealing irreversible changes in tissue. Interestingly, the cooling dependencies were different depending on the maximum

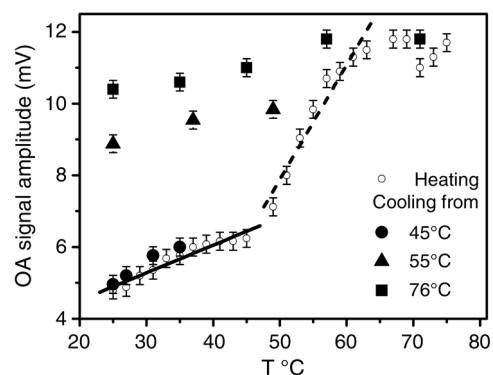


Fig. 3 An example of a temperature dependence of the OA signal amplitude in an *ex vivo* chicken breast sample. Open symbols correspond to heating, while solid symbols correspond to cooling regimes that start from different temperatures. The data points for the heating regime were least-square-fitted by two linear functions in the temperature ranges 25°C to 45°C (solid line) and 46°C to 63°C (dashed line).

temperature that the sample reached before cooling. Figure 3 shows two of these dependencies when cooling occurred, starting with over 70°C, and from 55°C.

3.2 Temperature Dependence of the OA Signal Amplitude in Porcine Lard

Figure 4 shows typical temperature dependencies of the OA signal for porcine lard during heating (open circles) and cooling (solid symbols). The main difference in the temperature dependence obtained for porcine lard from all other investigated tissues is that the amplitude of the OA signal decreases with increasing of temperature from 25°C to 76°C. In the case of sample cooling starting from any temperature above 36°C, the slope of the dependence changed and became less steep than that for heating. It may indicate that a partial change in fatty tissue structure occurs at any temperature exceeding the temperature of a living organism.

3.3 Temperature Dependence of the OA Signal Amplitude in Porcine Liver

An important characteristic of liver tissue is that it is richly perfused. Blood is the main absorber in the visible and near-IR range of optical radiation, and hemoglobin is known to transform at higher temperatures (above 60°C) into methemoglobin, which has higher optical absorption.^{26,36,56} Since the OA signal amplitude is determined by $\mu_a \Gamma$, its temperature dependence in liver should contain additional growth at high temperatures due to the change in absorption.

Figure 5 shows an example of temperature dependence of the OA signal amplitude for porcine liver. Similarly to muscle tissue, two linear dependencies are observed during heating, corresponding to pre- and post-coagulation. An additional growth in the OA signal amplitude occurs at temperatures above 72°C. When cooling of the samples had been performed starting with temperatures below 45°C, the dependence repeated the heating curve in the inverse direction. If the cooling process had started at temperatures larger than 45°C, the dependence was linear, but less steep than that for the heating process. The amplitude of the OA signal that was measured before heating, at room temperature, differed from that obtained after sample cooling from 80°C to room temperature by more than 200%.

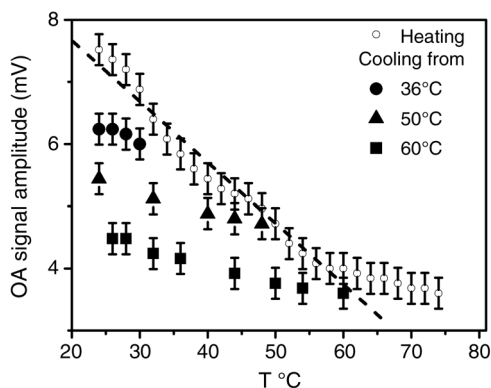


Fig. 4 An example of a temperature dependence of the OA signal amplitude in an *ex vivo* porcine lard sample. Open symbols correspond to heating, while solid symbols correspond to cooling regimes that start from different temperatures. The data points for the heating regime were least-square-fitted by a linear function (dashed line).

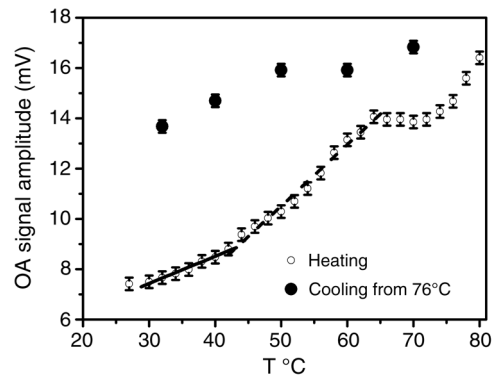


Fig. 5 An example of a temperature dependence of the OA signal amplitude in an *ex vivo* porcine liver sample. Solid symbols correspond to heating, while open symbols correspond to cooling. The data points for the heating regime were least-square-fitted by two linear functions in the temperature ranges 25°C to 42°C (solid line) and 42°C to 62°C (dashed line).

This result corresponds well to our earlier work,²¹ in which the optical properties of raw and boiled porcine liver tissues were measured.

3.4 Estimation of the Accuracy of Temperature Reconstruction in Tissue

Using the temperature dependence of the OA signal amplitude for different tissues, the accuracy of temperature reconstruction from the OA signal amplitude can be assessed. For that purpose, the obtained experimental dependencies in heating regime for each tissue type were divided into groups corresponding to temperature ranges in which the dependence is close to linear. In each of the selected temperature ranges, the data were least-square-fitted by a linear function, as shown in Figs. 3–5. For example, the dependencies for porcine liver and chicken breast samples were divided into two sections: 23°C to 45°C and 46°C to 65°C. Temperature dependencies of the OA signal amplitude for porcine fatty tissue samples were fitted with the linear function within the entire temperature range, since the experimental curves for this tissue did not reveal the change in slope.

Table 1 Linear fit of the temperature dependencies of the OA signal amplitude for chicken breast, porcine lard, and porcine liver samples. The results are averaged over 10 samples of each tissue type. The inaccuracy of temperature reconstruction using the mean slope is estimated for each temperature range.

Tissue type	Temperature range (°C)	Mean slope (mV/°C)	Standard deviation of the mean slope (mV/°C)	Inaccuracy of temperature reconstruction (%)
Chicken breast	25 to 45	0.069	0.008	10
	45 to 63	0.26	0.002	8
Porcine lard	25 to 65	0.098	0.005	5
Porcine liver	25 to 42	0.087	0.006	7
	42 to 62	0.26	0.003	11

The linear slopes mentioned above varied slightly from sample to sample within the same tissue type. The mean linear slope averaged over 10 samples for each tissue type is presented in Table 1, along with the standard deviation observed in the considered group of samples. The standard deviation from the mean slope was used to estimate the corresponding error in temperature reconstruction in case mean linear dependence was being used. As seen from Table 1, the error does not exceed 11%.

4 Discussion and Conclusions

In the present work, the dependence of the OA signal amplitude on tissue temperature was investigated in a wide range of temperatures (23°C to 80°C) for several different tissue types to obtain calibration curves $\mu_a \Gamma(T)$ for temperature monitoring during thermal therapies. Below, we will discuss the observed experimental facts in terms of changes in tissue structure and determine factors that may contribute to such dramatic changes in OA conversion efficiency during thermal impact. Multiple factors, namely the temperature dependencies of sound speed, specific heat, volume thermal expansion coefficient, and light absorption, can potentially influence the measured value of the OA signal amplitude. Unfortunately, not all these dependences are known from the literature; moreover, some of the dependences obtained by different authors demonstrate opposite trends (for example, changes in light absorption).^{34,43}

For the first, reversible, heating phase of chicken breast and porcine liver tissues (the temperature range of 23°C to 45°C) the growth of the OA signal amplitude with temperature is almost linear, with mean slopes of 0.069 mV/°C and 0.087 mV/°C, respectively. Most of the literature on the temperature behavior of the specific heat of water and muscle and liver tissues report very little changes before the coagulation threshold¹⁰ is reached, even in comparison with changes in sound speed, which do not exceed a few percent.^{9–13} Changes in the optical properties (light absorption and scattering) are also unlikely in this temperature range, due to absence of the irreversible changes in tissue structure. This statement is confirmed in our measurements: first, the temperature dependence of the OA signal amplitude does not exhibit hysteresis (see Fig. 3); second, the slope of the OA signal trailing edge changes very little in this region, which indicates no considerable changes in light distribution inside tissue samples and therefore no noticeable changes in tissue optical properties.

Thus, the only remaining parameter that may contribute to the change in OA conversion efficiency in liver and chicken breast tissues in the temperature range of 23°C to 45°C is the thermal expansion coefficient. It is known that the thermal expansion coefficient of liver and muscle tissues is much larger than that of water, but its temperature variation is much smaller than that of water.¹⁰ Indeed, within the temperature range of 23°C to 45°C, the increase of the amplitude of the OA signal excited in pure water would be 2.6 and 3.3 times faster than that in chicken breast and porcine liver tissues, respectively. This suggests that the main contribution to the temperature dependence of OA conversion before tissue coagulation threshold is the change in thermal expansion of water contained in tissue—72% to 75% reported for liver and muscle.⁶

A more dramatic increase in OA signal amplitude in the heating regime is observed for porcine liver and chicken breast tissues within the higher temperature range of 46°C to 65°C corresponding to the tissue coagulation zone. Interestingly, although the absolute value of the OA signal amplitude is larger

for the liver, the mean slope of the temperature dependences, averaged over 10 samples of each tissue type (see Table 1), is the same for both tissues—richly perfused liver and chicken breast, which contains far less blood. Therefore, it is unlikely that the OA signal amplitude growth is due to the increase in μ_a caused by structural changes in blood itself. However, both optical coefficients of tissue, μ_a and μ_s' , can change due to tissue dehydration, shrinking, and, consequently, the increase of the concentration of chromophores.^{40,41} Our measurements support this hypothesis: the duration of the OA signal is decreasing, and the trailing edge is becoming considerably steeper in this temperature range. This is clearly illustrated in Fig. 2(a) if one compares the OA signal profiles at 46°C and 56°C. This means that μ_{eff} of tissues is definitely increasing, but, unfortunately, the temporal profiles of OA signals detected in the backward mode do not allow the determination of the relative contributions of μ_a and μ_s' .

Dehydration of tissue during its coagulation may affect not only tissue optical coefficients, but Γ as well. The quantitative information on tissue dehydration during its thermal coagulation is scarce, and most of what is available comes from food science literature. In particular, intact skeletal muscle and liver tissues contain up to 75% water, and about 9% is lost during thermal denaturation.⁵⁷ Since the thermal expansion coefficient of soft tissues exceeds that for water by more than two times,¹⁰ tissue dehydration could lead to the increase of β . Furthermore, dehydration also noticeably decreases the specific heat of tissues. For example, the reported experimental values for c_p of hydrated and 18% dehydrated collagen are 1790 J/kg/K and 1560 J/kg/K, respectively.¹⁰ According to Cooper and Trezek,⁵⁸ the specific heat of soft tissues can be estimated as a mass fractional sum of the specific heat of water (4200 J/kg/K), solid protein tissue (1560 J/kg/K), and fat, which corresponds well to the specific heat reported for intact liver and muscle tissue: $c_p = 3300$ to 3600 J/kg/K. The 9% water loss that occurs with coagulation thus would cause the decrease in tissue-specific heat that would result in a 10% increase in OA signal amplitude. This means that the value of β/c_p could change significantly during tissue coagulation. The values of the speed of sound in water and in soft tissues differ by no more than 6%; hence, they should not change significantly with tissue denaturation and dehydration.

To summarize the above, we speculate that the main reason for a sharp increase of OA conversion efficiency for liver and muscle tissues in the temperature range of 46°C to 65°C is most probably associated with dehydration, causing dramatic increase in the value of β/c_p and, possibly, some increase in μ_a due to the change in the concentration of chromophores.

The temperature range of 65°C to 75°C most probably represents the heating of completely coagulated tissue. The behavior of the OA signal amplitude is markedly different for chicken breast tissue, in which the OA signal amplitude does not change within the experimental error, and porcine liver tissue, in which it starts to increase from 72°C. The slope of the trailing edge of the OA signal does not change in chicken breast tissue either, but it undergoes a significant steepening in porcine liver at temperatures over 72°C. We believe that this fact can be explained by formation of methemoglobin in blood, which leads to the increase of μ_a . Temperatures at which formation of methemoglobin were observed differ between literature sources within the range 60°C to 70°C^{26,36,56} and are reported to depend on sample preparation, blood oxygenation, and other experimental conditions. Note also that the absolute value of the OA signal

amplitude for porcine liver is much larger than that for chicken muscle at any given temperature, due to the presence of blood in the liver structure.

The components of the Gruneisen coefficient in this temperature range are likely to remain constant. The dependence $\beta(T)$ should become much weaker in both tissues since the tissue is already dehydrated, and the water content is thought to provide the main contribution into the growth of the thermal expansion coefficient with temperature. Within this temperature range, the value of c_0 is reported to decrease slightly with temperature,¹¹ and c_p remains virtually unchanged.³⁷

Cooling of both muscle and liver tissues does not change either their water content or their optical properties. Therefore, the slopes of temperature dependences of the OA signal amplitude during tissue cooling should mainly follow the dependence of $\beta(T)$ inherent to the current stage of tissue dehydration. Therefore, if the temperature at which the cooling starts is below $\sim 45^\circ\text{C}$, the OA conversion efficiency returns to its initial value at the initial temperature. When the tissue is cooled from temperatures exceeding the denaturation threshold, the OA conversion efficiency exhibits a hysteresis; i.e., it does not return to the initial value after cooling down to the initial temperature.

To summarize, we believe that the main factors determining the increase of the OA conversion efficiency in muscle and liver tissues with temperature are (1) tissue dehydration leading to the change in the value of β/c_p ; (2) gradual changes in light absorption during tissue coagulation in the temperature range of 45°C to 65°C due to the increase in the concentration of chromophores;^{40,41} (3) increase in optical absorption in richly perfused tissues due to formation of methemoglobin at temperatures exceeding 70°C ; and (4) the dependence of $\beta(T)$, which is followed by the OA signal amplitude temperature dependence during the cooling process.

The OA conversion efficiency has a totally different behavior in cases of heating or cooling of porcine lard samples. As seen in Fig. 4, the OA signal amplitude decreases gradually with temperature during the heating process, and the dependence is close to linear. We believe that the main reason for that phenomenon is the negative slope of the curve $\beta(T)$ for this tissue type.¹⁰ Slight changes in sound speed¹¹ cannot be responsible for the observed twofold decrease of the OA signal amplitude. The dependence of $c_p(T)$ for fat was studied by Choi and Okos,⁵⁹ where it was shown to be smooth and weak ($\sim 1\%$ per 10°C). There is no obvious reason for changes in optical coefficients with temperature; indeed, the slope of the OA signal trailing edge remains the same over the entire temperature range [Fig. 2(b)].

Explanation of the behavior of the OA conversion in lard tissue during cooling is the most challenging among the dependencies observed in this study. As reported by Duck,¹⁰ phase transitions in purified fats exist in the considered temperature range, and the positions of the transition points vary considerably for different fats. Since fatty tissue compositions may vary from sample to sample and contain impurities, these phase transitions may merge and/or shift and are known to irreversibly change the specific heat of fatty tissue and, possibly, its thermal expansion coefficient.¹⁰ Most probably, this is the reason for the hysteresis observed in our measurements if the lard samples were heated up to temperatures exceeding 36°C ; the full description of this phenomenon in terms of structural changes in fatty tissue could be the goal of a separate study.

The temperature dependencies of the OA conversion efficiency in some of the tissues, in limited temperature ranges,

were reported earlier by Larin et al.,⁴⁴ Pramanik and Wang,⁴⁶ and Shah et al.⁴⁷ In particular, within the temperature range below the tissue coagulation threshold, the relative change of the OA signal amplitude in liver and muscle tissues correspond well to the values reported by Larin et al.⁴⁴ and are much lower than these observed by Pramanik and Wang,⁴⁶ and Shah et al.⁴⁷ in porcine and turkey muscle tissues. In the higher temperature range (45°C to 65°C) we observed considerably smaller relative changes of OA signal amplitude for muscle and liver tissues (see Figs. 3 and 5) than these reported by Larin et al.⁴⁴ Most probably, this is due to the use of a narrow laser beam in presented measurements, which were thereby not affected by the increase in light scattering during coagulation. Quantitative data characterizing OA conversion efficiency in fatty tissue in the broad temperature range were most probably obtained for the first time (Fig. 4).

To conclude, in the present paper, the calibration dependencies of OA conversion efficiency on tissue temperature, $\mu_a\Gamma$, were obtained for several different tissue types in the temperature range of 20°C to 80°C . These dependencies will be used in future *in vitro* and *in vivo* experiments to reconstruct temperature maps during tissue heating; for example, by HIFU transducers. The obtained calibration curves most probably will need to be corrected for *in vivo* studies. However, the fact of the presence of a plateau in the temperature dependence of OA conversion efficiency at the temperatures above 60°C , illustrating the end of tissue coagulation, may be used directly as an indicator for completeness of a thermal therapy, which is also very important in clinical applications. We hope that the obtained results will be useful for the development of the OA methods and devices for *in vivo* temperature monitoring in biological tissues.

Acknowledgments

This work was partially supported by the Russian Foundation for Basic Research (Projects No. 07-02-00940-a, 10-02-01468-a) and the International Science and Technology Center (Project No. 3691).

References

1. F. Wu et al., "Advanced hepatocellular carcinoma: treatment with high-intensity focused ultrasound ablation combined with transcatheter arterial embolization," *Radiology* **235**(2), 659–667 (2005).
2. G. Aus, "Current status of HIFU and cryotherapy in prostate cancer: a review," *Eur. Urol.* **50**(5), 927–934 (2006).
3. X. L. Ren et al., "Extracorporeal ablation of uterine fibroids with high-intensity focused ultrasound: imaging and histopathologic evaluation," *J. Ultrasound Med.* **26**(2), 201–212 (2007).
4. T. J. Dubinsky et al., "High-intensity focused ultrasound: current potential and oncologic applications," *Am. J. Roentgenol.* **190**(1), 191–199 (2008).
5. R. Viard et al., "Determination of the lesion size in laser-induced interstitial thermal therapy (LITT) using a lowfield MRI," in *Proc. 29th Annual Intl. Conf. IEEE EMBS*, pp. 214–217, IEEE, Lyon (2007).
6. R. L. Nasoni et al., "In vivo temperature dependence of ultrasound speed in tissue and its application to noninvasive temperature monitoring," *Ultra. Imaging* **1**(1), 34–43 (1979).
7. C. H. Farny and G. T. Clement, "Ultrasound phase contrast thermal imaging with reflex transmission imaging methods in tissue phantoms," *Ultra. Med. Biol.* **35**(12), 1995–2006 (2009).
8. P. R. Stepanishen and K. C. Benjamin, "Forward and backward projection of acoustic fields using FFT methods," *J. Acoust. Soc. Am.* **71**(4), 803–812 (1982).
9. J. Bamber and C. Hill, "Ultrasonic attenuation and propagation speed in mammalian tissues as a function of temperature," *Ultra. Med. Biol.* **5**(2), 149–157 (1979).

10. F. A. Duck, *Physical Properties of Tissue*, Academic Press, London (1990).
11. B. Rajagopalan et al., "Variation of acoustic speed with temperature in various excised human tissues studied by ultrasound computerized tomography," in *Ultrasonic Tissue Characterization Special II. Publication. National Bureau of Standards M. Linzer, Ed.*, Government U. S. Printing Office, Washington, D.C., 227–233 (1979).
12. G. Ghoshal et al., "Temperature-dependent ultrasonic characterization of biological media," *J. Acoust. Soc. Am.* **130**(4), 2203–2211 (2011).
13. U. Techavipoo et al., "Temperature dependence of ultrasonic propagation speed and attenuation in excised canine liver tissue measured using transmitted and reflected pulses," *J. Acoust. Soc. Am.* **115**(6), 2859–2865 (2004).
14. M. O. Köhler et al., "Spectrally selective pencil-beam navigator for motion compensation of MR-guided high-intensity focused ultrasound therapy of abdominal organs," *Mag. Res. Med.* **66**(1), 102–111 (2011).
15. H. Furusawa et al., "Magnetic resonance-guided focused ultrasound surgery of breast cancer: reliability and effectiveness," *J. Amer. Coll. Surg.* **203**(1), 54–63 (2006).
16. D. Gianfelice et al., "Feasibility of magnetic resonance imaging-guided focused ultrasound surgery as an adjunct to tamoxifen therapy in high-risk surgical patients with breast carcinoma," *J. Vasc. Intervent. Radiol.* **14**(10), 1275–1282 (2003).
17. F. A. Taran et al., "Magnetic resonance-guided focused ultrasound (MRgFUS) compared with abdominal hysterectomy for treatment of uterine leiomyomas," *Ultrasound. Obstet. Gynecol.* **34**(5), 572–578 (2009).
18. R. J. Stafford et al., "Laser-induced thermal therapy for tumor ablation," *Crit. Rev. Biomed. Eng.* **38**(1), 79–100 (2010).
19. K. Kuroda, "Non-invasive MR thermography using the water proton chemical shift," *Int. J. Hyperthermia* **21**(6), 547–560 (2005).
20. J. Welch and M. J. C. van Gemert, *Optical-Thermal Response of Laser-Irradiated Tissue*, Plenum, New York (1995).
21. T. D. Khokhlova et al., "Opto-acoustic diagnostics of the thermal action of high-intensity focused ultrasound on biological tissues: the possibility of its applications and model experiments," *Quant. Elec.* **36**(12), 1097–1102 (2006).
22. A. M. K. Nilsson et al., "Changes in spectral shape of tissue optical properties in conjunction with laser-induced thermotherapy," *Appl. Opt.* **37**(7), 1256–1267 (1998).
23. M. Ben-David et al., "Measuring tissue heat penetration by scattered light measurements," *Laser Surg. Med.* **40**(7), 494–499 (2008).
24. R. Agah et al., "Dynamics of temperature dependent optical properties of tissue: dependence on thermally induced alteration," *IEEE Trans. Biomed. Eng.* **43**(8), 839–846 (1996).
25. B. Soroushian, W. M. Whelan, and M. C. Kolios, "Study of laser-induced thermoelastic deformation of native and coagulated *ex-vivo* bovine liver tissues for estimating their optical and thermomechanical properties," *J. Biomed. Opt.* **15**(6), 065002 (2010).
26. L. L. Randeberg et al., "Methemoglobin formation during laser induced photothermolysis of vascular skin lesions," *Laser Surg. Med.* **34**(5), 414–419 (2004).
27. V. V. Tuchin, *Handbook of Optical Biomedical Diagnostics*, SPIE Press, Bellingham, WA (2007).
28. T. W. Murray et al., "Detection of ultrasound-modulated photons in diffuse media using the photorefractive effect," *Opt. Lett.* **29**(21), 2509–2511 (2004).
29. P. Lai et al., "Real-time monitoring of high-intensity focused ultrasound lesion formation using acousto-optic sensing," *Ultra. Med. Biol.* **37**(2), 239–252 (2011).
30. V. E. Gusev and A. A. Karabutov, *Laser Optoacoustics*, American Institute of Physics, New York (1993).
31. H. Li and L. V. Wang, "Photoacoustic tomography and sensing in biomedicine," *Phys. Med. Biol.* **54**(19), R59–R97 (2009).
32. R. A. Kruger et al., "Thermoacoustic computed tomography using a conventional linear transducer array," *Med. Phys.* **30**(5), 856–860 (2003).
33. T. D. Khokhlova, I. M. Pelivanov, and A. A. Karabutov, "Methods of optoacoustic diagnostics of biological tissues," *Acoust. Phys.* **55**(4–5), 674–684 (2009).
34. K. Giering et al., "Review of thermal properties of biological tissues," in *Laser-induced Interstitial Thermotherapy*, G. Müller and A. Roggan, Eds., SPIE Opt. Eng. Press, Bellingham, WA (1995).
35. J. P. Ritz et al., "Continuous changes in the optical properties of liver Tissue during laser-induced interstitial thermotherapy," *Laser Surg. Med.* **28**(4), 307–312 (2001).
36. J. Lee et al., "Noninvasive *in vivo* monitoring of methemoglobin formation and reduction with broadband diffuse optical spectroscopy," *J. Appl. Physiol.* **100**(2), 615–622 (2006).
37. D. Haemmericha et al., "In vitro measurements of temperature-dependent specific heat of liver tissue," *Med. Eng. Phys.* **28**(2), 194–197 (2006).
38. A. F. Emery and K. M. Sekins, "Thermal science for physical medicine," in *Therapeutic Heat and Cold*, J. F. Lehmann, Ed., Williams and Wilkins, Baltimore, MD (1982).
39. C. Simon, P. VanBaren, and E. Ebbini, "Two-dimensional temperature estimation using diagnostic ultrasound," *IEEE Trans. Ultrason. Ferroelectrics Freq. Contr.* **45**(4), 1088–1099 (1998).
40. A. N. Yaroslavsky et al., "Optical properties of selected native and coagulated human brain tissues *in vitro* in the visible and near infrared spectral range," *Phys. Med. Biol.* **47**(12), 2059–2073 (2002).
41. I. F. Cilesiz and A. J. Welch, "Light dosimetry: effects of dehydration and thermal damage on the optical properties of the human aorta," *Appl. Opt.* **32**(4), 477–487 (1993).
42. J. F. Black, N. Wade, and J. K. Barton, "Mechanistic comparison of blood undergoing laser photocoagulation at 532 and 1,064 nm," *Laser Surg. Med.* **36**(2), 155–165 (2005).
43. J. P. Ritz et al., "Optical properties of native and coagulated human liver tissue and liver metastases in the near infrared range," *Laser Surg. Med.* **23**(4), 194–203 (1998).
44. K. V. Larin, I. V. Larina, and R. O. Esenaliev, "Monitoring of tissue coagulation during thermotherapy using optoacoustic technique," *J. Phys. D: Appl. Phys.* **38**(15), 2645–2653 (2005).
45. P. V. Chitnis et al., "Feasibility of optoacoustic visualization of high-intensity focused ultrasound-induced thermal lesions in live tissue," *J. Biomed. Opt.* **15**(2), 021313 (2010).
46. M. Pramanik and L. V. Wang, "Thermoacoustic and photoacoustic sensing of temperature," *J. Biomed. Opt.* **14**(5), 054024 (2009).
47. J. Shah et al., "Photoacoustic imaging and temperature measurement for photothermal cancer therapy," *J. Biomed. Opt.* **13**(3), 034024 (2008).
48. A. A. Karabutov et al., "Backward detection of laser-induced wide-band ultrasonic transients with optoacoustic transducer," *J. Appl. Phys.* **87**(4), 2003–2014 (2000).
49. A. Tam, "Applications of photoacoustic sensing technologies," *Rev. Mod. Phys.* **58**(2), 381–429 (1986).
50. C. M. Gardner, S. L. Jacques, and A. J. Welch, "Light transport in tissue: accurate expressions for one-dimensional fluence rate and escape function based upon Monte Carlo simulation," *Lasers Surg. Med.* **18**(2), 129–138 (1996).
51. P. S. Grashin et al., "Distribution of the laser radiation intensity in turbid media: Monte Carlo simulations, theoretical analysis, and results of optoacoustic measurements," *Quant. Elec.* **32**(10), 868–874 (2002).
52. I. M. Pelivanov et al., "Opto-acoustic measurement of the local light absorption coefficient in turbid media," *Quant. Elec.* **39**(9), 830–838 (2009).
53. M. B. Vinogradova, O. V. Rudenko, and A. P. Sukhorukov, *Wave Theory*, Nauka, Moscow (1979).
54. L. V. Wang, *Photoacoustic Imaging and Spectroscopy*, CRC Press, New York (2009).
55. I. M. Pelivanov et al., "Direct opto-acoustic *in vitro* measurement of the spatial distribution of laser radiation in biological media," *Quant. Elec.* **36**(12), 1089–1096 (2006).
56. J. F. Black and J. K. Barton, "Chemical and structural changes in blood undergoing laser photocoagulation," *Photochem. Photobiol.* **80**(1), 89–97 (2004).
57. R. Y. Murphy and B. P. Marks, "Effect of meat temperature on proteins, texture and cook loss for ground chicken breast patties," *Poult. Sci.* **79**(1), 99–104 (2000).
58. T. E. Cooper and G. J. Trezek, "Correlation of thermal properties of some human tissues with water content," *Aerosp. Med.* **42**(1), 24–28 (1971).
59. Y. Choi and M. R. Okos, "Effects of temperature and composition on the thermal properties of food," in *Food Engineering and Process Applications*, Vol. 1, M. Le Maguer and P. Jelen, Eds., Elsevier, London (1986).